Isotopic and spin selectivity of H_2 adsorbed in bundles of carbon nanotubes

February 1, 2008

R.A. Trasca, M.K. Kostov and M.W. Cole
Department of Physics, The Pennsylvania State University, University Park, PA 16802

Abstract

Due to its large surface area and strongly attractive potential, a bundle of carbon nanotubes is an ideal substrate material for gas storage. In addition, adsorption in nanotubes can be exploited in order to separate the components of a mixture. In this paper, we investigate the preferential adsorption of D_2 versus H_2 (isotope selectivity) and of ortho versus para (spin selectivity) molecules confined in the one-dimensional grooves and interstitial channels of carbon nanotube bundles. We perform selectivity calculations in the low coverage regime, neglecting interactions between adsorbate molecules. We find substantial spin selectivity for a range of temperatures up to 100 K, and even greater isotope selectivity for an extended range of temperatures, up to 300 K. This isotope selectivity is consistent with recent experimental data, which exhibit a large difference between the isosteric heats of D_2 and H_2 adsorbed in these bundles.

1 Introduction

The adsorption of gases within single-walled, carbon nanotubes (SWNT) has recently attracted broad attention among physicists, chemists, materials scientists and engineers [42, 2, 3, 4, 5, 6, 7, 8, 9, 10, 11, 12, 13, 14, 15, 16, 17].

Experiments have shown that one can create ordered arrays of nanotubes [18, 19, 20, 21, 22], which form a close-packed bundle (or rope) of SWNT's. Ideal bundles of nanotubes consist of very long strands of nearly parallel tubes held together at equilibrium separation by intermolecular forces. The small diameter and large aspect ratio of the nanotubes make them interesting systems for gas adsorption. In such a bundle, physisorption may occur at four distinct sites: i) inside the tubes (endohedral adsorption); ii) in the interstitial channels (IC) between three contiguous nanotubes (exohedral adsorption); iii) in the grooves between adjacent nanotubes on the external surface of the bundle, and iv) elsewhere on the outside surface of the bundle. In this paper, we assess the ability of nanotube bundles to preferentially adsorb specific isotope and spin species.

Small atoms and molecules, in contrast to larger molecules, have been predicted to fit well in the ICs of a nanotube bundle [18, 23]. For such species, the IC's environment provides a large number of neighboring C atoms at nearly optimal distance from the adatom, so the interstitial binding energy is larger than is found in other known environments [16]. The grooves also present strongly attractive environments for both small and large molecules. The binding energies in these sites have been determined experimentally to be between 50 % and 100 % greater than the values on graphite [40, 42, 43, 37].

Molecular hydrogen inside SWNTs is a particularly appealing system to study, since its adsorption in ICs and grooves is relevant to both gas storage and isotope separation [25, 26, 30, 31]. "Selectivity" is the term used to describe the separation, or selective adsorption, of one species relative to the other species of a mixture. In a mixture of two components, the selectivity of component 1 relative to that of 2 is:

$$S = (x_1/x_2)/(y_1/y_2) \tag{1}$$

with $x_i(y_i)$ the pore (bulk) molar fractions. Since two isotopes have similar sizes, shapes and interaction potentials, the separation of isotopic mixtures is a difficult and energy-expensive process, requiring special experimental techniques, such as cryogenic distillation, diffusion separation, laser isotope separation or microwave molecular separation [27, 28, 29]. However, most of these processes have low selectivity for separating H_2 isotopes. Recently, a novel separation technique called quantum sieving was predicted to be particularly efficient for nanotubes [24, 25, 34, 45]. Quantum sieving separates lighter molecules from heavier ones by selectively adsorbing heavier molecules. Such

selective adsorption can be explained by the higher zero-point energy of the light species, which makes their adsorption relatively unfavorable. Quantum sieving can be implemented when the adsorbate is effectively confined to a one-dimensional (1D) channel or a 2D surface or a small cavity (0D). The selectivities observed for adsorption of H_2 isotopes on common substrates such as graphite, zeolites, and alumina are low - typically in the range of 1.1 to 3 [31, 32, 33]. However, differences in zero-point energies of the adsorbed species are expected to be particularly large when molecules are confined in very narrow pores. Wang *et al.* have shown that nanopores with diameters wider than 7 $\mathring{A}$ exhibit weak selectivity while smaller nanopores were predicted to exhibit large selectivities [24]. Carbon nanotubes typically have diameters larger than 7 $\mathring{A}$, but the interstitial channels are smaller, so that they have a pore size and solid-fluid potential which can effectively sieve mixtures of H_2 and D_2. Indeed, Path Integral Monte Carlo calculations at variable pressures [25] yielded large isotope selectivity in the IC. Our calculations are performed in the limit of low coverage (virtually zero pressure), using what we believe to be an improved gas-solid interaction potential.

The solid-fluid potential is usually modelled as a pair-wise sum of Lennard-Jones interactions between adatoms and carbon atoms [25, 26]. The potential used in our study is the one recently developed by Kostov *et al.* [35]. In addition to terms present in previous calculations, Kostov's potential includes also the interactions of the H_2 quadrupole moment with the local electrostatic field of C nanotubes (found from ab initio calculations [41]) and interactions of the H_2 static multipole moments with the image charges induced on the surrounding nanotubes. The model yields a strongly confining potential for H_2 and D_2, of depth about 1800 K ($\sim$ 160 meV), which alters the rotational spectrum and induces a large difference between isotopic zero point energies. As we will show, the calculated difference between H_2 and D_2 binding energies is consistent with recent isosteric heat data of Wilson *et al.* [37]. This large difference, when exponentiated in an Arrhenius expression at low temperature, yields huge isotope selectivities in the IC and groove, far exceeding that on common sorbents (e.g. graphite and zeolites).

The rotational hindrance of H_2 molecules adsorbed in carbon nanotube bundles is a controversial issue. There exist experiments showing no alteration of the rotational spectrum [38] and other experiments (with different samples) which manifest large changes compared to the free rotation energy spectrum [36]. The calculations of Kostov *et al.* indicate that interstitially adsorbed H_2 has a significantly hindered rotational motion [35, 36]. The exis-

tence of a large rotational barrier leads to large splittings and shifts (relative to an orientationally invariant potential) of the H_2 and D_2 rotational energy levels (see Fig.1). In this work we show that a consequence of this hindered rotational motion is a significant spin selectivity in the ICs and grooves.

Recently, Hathorn *et al.* showed that quantization of the restricted rotational motion of H_2 and D_2 confined in SWNTs contributes significantly to quantum sieving [45]. Their study, however, is substantially different from the present work, since they consider H_2 adsorbed within a single nanotube and approximate the rotational potential as that of the molecule on the axis of the nanotube. In addition, they employed a modified Lennard-Jones potential with ϵ and σ parameters far different from the potential parameters assumed in this work. They find significantly hindered rotational spectrum for the adsorbed molecule for small nanotubes. Their results are qualitatively consistent with our results although we are considering quite different sites.

The outline of this paper is as follows. In the next section, we calculate the ortho-para selectivity as a function of temperature (T), taking into account the hindered rotational motion. In Section III, we derive the specific heat due to the rotational motion of the adsorbed molecules. Section IV presents results for the isotope selectivity of mixtures of H_2 and D_2. Section V presents calculations of the isosteric heats of H_2 and D_2 and compares these with the experimental results of Wilson *et al.* [37]. Section VI summarizes and discusses this work.

2 Ortho-para selectivity

In order to compute the selectivity of component 1 (e.g. ortho) relative to component 2 (e.g. para) at low coverage, we use the equilibrium condition relating the chemical potential of each component of the 3D vapor(outside the nanotube bundles) to that of the 1D gas adsorbed in the IC:

$$\mu_i^{vapor} = \mu_i^{IC} \tag{2}$$

where i stands for each component, ortho and para. We employ statistical mechanics to find the chemical potential $\mu = (\partial F/\partial N)_{T,V}$, where $F = -k_B T \ln Q$ is the Helmholtz free energy, Q is the canonical partition function and k_B is Boltzmann's constant. In the low density limit, the partition function involves energy contributions from (hindered) rotation, vibration and

from translation of the center of mass (CM) in the presence of a transverse confining potential.

In the IC or groove, the molecules are assumed to move freely along the axial direction, so the fluid is described by a constant(mean) 1D density, ρ. The effect of corrugation on the motion is sensitive to assumptions about registry of adjacent tubes [46, 47] and is neglected here. The CM transverse oscillation is described by the one-particle partition function, q^{cm}. The internal degrees of freedom consist of the intra-molecular vibrations and hindered rotations, described by q^{vib} and q^{rot}, respectively. Therefore:

$$F_i^{IC} = -Nk_BT \ln[\frac{e}{\rho_i \lambda} q_i^{cm} q_i^{vib} (g_i q_i^{rot}) \exp(-C_i/(k_BT))] \tag{3}$$

$$\mu_i^{IC} = C_i - k_BT \ln(\frac{e}{\rho_i \lambda}) - k_BT \ln q_i^{cm} - k_BT \ln q_i^{vib} - k_BT \ln (g_i q_i^{rot}) \tag{4}$$

where i stands for para and ortho, $\lambda = \sqrt{2\pi\hbar^2/(mk_BT)}$, g_i is the nuclear spin degeneracy and C_i is the interaction energy experienced by molecules due to the confining environment.

The partition function of the coexisting gas outside the nanotube bundle has contributions from the 3D translation motion and from internal degrees of freedom (vibration and free rotation of the molecules). The free energy and the chemical potential are then:

$$F_i^{vapor} = -Nk_BT \ln[\frac{e}{n_i \lambda^3} q_i^{vib} (g_i q_i^{free})] \tag{5}$$

$$\mu_i^{vapor} = -k_BT \ln \frac{e}{n_i \lambda^3} - k_BT \ln q_i^{vib} - k_BT \ln (g_i q_i^{free}) \tag{6}$$

where n_i is the 3D density of ortho or para vapor outside the nanotube bundle.

Experimental data of Williams *et al* and calculations of Kostov *et al* indicate that the intra-molecular vibrations are essentially the same in the IC as in free space [23, 44]. The CM oscillations depend only on the molecular mass, so they give the same contribution to the ortho and para partition functions. Finally, the only relevant contributions to the spin selectivity come from the even and odd rotational partition functions, denoted q_+ and q_-, respectively:

$$q_+ = \sum_{j=even} \sum_{m=-j}^{j} g_{jm} \exp(-\beta \epsilon_{jm}) \tag{7}$$

where $\beta = 1/(k_B T)$, g_{jm} is the rotational degeneracy (not including the nuclear degeneracy), and ϵ_{jm} are the rotational levels. For the odd partition function (q_-), the summation in $Eq.7$ is done only over the odd rotational levels. In free space, both H_2 and D_2 can be modelled as free quantum rotors with $g_{jm} = j(j+1)$ and $\epsilon_{jm} = j(j+1)B$. Here j is the rotational quantum number and $B = \hbar^2/(2I)$, the rotational constant of H_2 or D_2. However, the different character of the nuclear spin (fermionic for H_2 and bosonic for D_2) imposes different conditions on the total wavefunction (antisymmetric for H_2 and symmetric for D_2), so that the nuclear degeneracies corresponding to even and odd rotational states are different: $g_+^{H_2} = 1$, $g_-^{H_2} = 3$ and $g_+^{D_2} = 6$, $g_-^{D_2} = 3$. By convention, the name ortho is given to the species with larger statistical weight, so the even states are called para for H_2 and ortho for D_2. Thus, at high T, the ortho and para molecules exist in the ratio of 3:1 in the case of H_2 and 6:3 in the case of D_2.

The spin selectivity in the low coverage (pressure) limit involves a ratio of densities, which can be found by imposing the equilibrium condition ($Eq.2$):

$$S = \frac{(\rho_-/\rho_+)_{IC}}{(n_-/n_+)_{vapor}} \tag{8}$$

where $-$ and $+$ subscripts correspond to the odd and even rotational states, respectively (ortho and para for H_2, para and ortho for D_2). All similar factors mentioned previously cancel out in S and, in the end, the low coverage selectivity depends on just the even and odd partition functions, q_+ and q_-:

$$S = \frac{(q_-^{IC}/q_+^{IC})}{(q_-^{vapor}/q_+^{vapor})} \tag{9}$$

A qualitative understanding of the spin selectivity can be achieved by examining the rotational spectrum. The ortho-para ratio in the IC, in the limit of high T, is the same as in the gas phase. But since the energy spectrum changes in the IC, the overall partition functions differ, with particularly large effects at low T. Fig.1 contrasts the rotational spectra of H_2 in the IC (as computed by Kostov) and in free space. In the IC, the reference energy is the energy the molecule would have if it does not rotate (C_{H_2}=-1275 K)[48]. Notice that the ground (para) state is shifted down from this value by ~ 200 K and the first excited state (ortho $j = 1, m_j = 0$) is also shifted down ($\sim 60\ K$), close to the ground state. The D_2 rotational spectrum undergoes a similar alteration in the IC, but with a smaller shift of the ground (ortho)

state (about 130 K) with respect to a different reference energy (C_{D_2}=-1445 K), and a slightly larger excitation energy to the ($j = 1, m_j = 0$) para state (about 85 K)[49]. The shift in the first excited state (ortho for H_2, para for D_2) towards the ground state (para for H_2, ortho for D_2) causes the ortho to para ratio of H_2 molecules, or para to ortho ratio of D_2 molecules, to increase substantially in the IC with respect to that in free space. In the groove site, these ratios are still larger than in free space, but smaller, however, than in the IC, due to the lesser confinement between the two nanotubes in the groove site. At low T, all but the lowest states yield negligible contributions to q^{rot}, so that the selectivity depends only on the values of the lowest excitation energies in the IC and free space.

$$S_o = \frac{\exp[-\beta(\epsilon_{10} - \epsilon_{00})] + 2\exp[-\beta(\epsilon_{11} - \epsilon_{00})]}{3\exp[-2\beta B]} \tag{10}$$

where the free space separation is twice the rotational constant B=85 K for H_2.

The results for the ortho-para selectivity are shown in Fig.2. We find that the spin selectivity is larger than 1 for an extended range of temperatures, up to 100 K in the IC and $\sim$ 75 K in grooves. This is consistent with the difference between the excitation energies in the IC (groove) and in free space which enters *Eq.*10. As discussed above, the alterations of the rotational spectrum favor the H_2 ortho species, whereas for D_2, the para molecules are preferentially adsorbed. Since the H_2 molecules have a larger zero point motion than D_2 molecules, they experience more rotational hindrance and their spectrum is more altered in the corresponding energy scale. Since the reference energy does not count for the spin selectivity, this exhibits larger values for H_2 than for D_2.

3 Rotational specific heat

In order to compute the thermodynamic properties of the adsorbate, one works with the composite equilibrium partition function:

$$q_{rot}^{H_2} = S(2S+1)q_+ + (S+1)(2S+1)q_- \tag{11}$$

$$q_{rot}^{D_2} = (S+1)(2S+1)q_+ + S(2S+1)q_- \tag{12}$$

where $S = 1/2$ for H_2 and $S = 1$ for D_2. We will discuss the H_2 case and point out the differences in the case of D_2. In many circumstances,

H_2 is not in thermal equilibrium as regards the relative magnitudes of para and ortho components, because the probability of flipping the nuclear spin is very small (the lifetime in free space is $\sim$ one year). Therefore, the transition probability of a molecule from one nuclear spin state to another is negligible during a specific heat experiment. Consequently, the sample may be viewed as a non-equilibrium mixture of two independent species, which give additive contributions to the heat capacity.

$$C_{non-eq} = f_p C_p + f_o C_o \tag{13}$$

Here f_p and f_o are the para and ortho molar fractions. In an equilibrium mixture these depend on temperature, whereas in a non-equilibrium mixture their relative concentrations are determined by the initial conditions. In our calculations, we let the para and ortho molar fractions have their high T values: $f_p = 1/4$ and $f_o = 3/4$. The para and ortho specific heats (in the low density limit) are:

$$C_{p,o} = N_{p,o} k_B \frac{d}{dT}(T^2 \frac{d}{dT} \ln q_{+,-}) \tag{14}$$

At low T, only the lowest levels contribute to the specific heat. Let us consider only the first two levels: ϵ_{00} and ϵ_{20} for the para species, and ϵ_{10} and ϵ_{11} for the ortho species. Applying the formulae above, the para and ortho specific heats are:

$$C_p = N k_B \frac{(\epsilon_{20} - \epsilon_{00}) e^{-\beta(\epsilon_{20} - \epsilon_{00})}}{(1 + e^{-\beta(\epsilon_{20} - \epsilon_{00})})^2} \tag{15}$$

$$C_o = N k_B \frac{2(\epsilon_{11} - \epsilon_{10}) e^{-\beta(\epsilon_{11} - \epsilon_{10})}}{(1 + 2e^{-\beta(\epsilon_{11} - \epsilon_{10})})^2} \tag{16}$$

Thus, at low T, the para and ortho heats in the IC depend only on the excitation energies $(\epsilon_{20} - \epsilon_{00})$ and $(\epsilon_{11} - \epsilon_{10})$, respectively. Fig. 3 (a,b) shows a comparison between the para, ortho and non-equilibrium specific heats in free space and in the IC. Notice that, at low T, in the IC the main contribution to the net specific heat comes from C_o, whereas in free space it comes from C_p. This is related to the finite excitation energy $(\epsilon_{11} - \epsilon_{10})$ between (j=1) ortho states in IC, which are degenerate in free space (see fig.1). It can be shown that the peak in the heat capacity occurs at $T \approx \Delta/(3k_B)$, where Δ is the first excitation energy present in a specific problem. Therefore, in free space the para peak is at about 80 K, while in the IC the ortho peak is at about 75 K.

In some environments, however, the ortho-para conversion may occur quickly (e.g. due to magnetic impurities). In this case, the net rotational specific heat is obtained from the composite partition function ($Eqs.11, 12$):

$$C_{eq} = Nk_B \frac{d}{dT}(T^2 \frac{d}{dT} \ln q_{rot}) \tag{17}$$

At low T, the equilibrium specific heat depends only on the $(\epsilon_{10} - \epsilon_{00})$ excitation energy:

$$C_{eq} = Nk_B \frac{(\epsilon_{10} - \epsilon_{00}) e^{-\beta(\epsilon_{10} - \epsilon_{00})}}{(1 + e^{-\beta(\epsilon_{10} - \epsilon_{00})})^2} \tag{18}$$

The equilibrium specific heats of H_2 and D_2 in the IC are shown in Fig.4. In the case of H_2, there is a substantial ortho-para conversion peak at about 20 K, followed by a gentle rise above 75 K, corresponding to ortho-ortho excitation. However, in the case of D_2, the ortho-para conversion appears only as a small bump at about 25 K, since the molar weights of para and ortho species are now different. At high T, the rotational specific heat per molecule goes to k_B, the classical result for a free rotor.

4 Isotope slectivity

Let us now consider a mixture of H_2 and D_2. The equilibrium condition between the 1D gas adsorbed in the ICs or grooves and the coexisting vapor outside the nanotube bundles is given again by $Eq.2$: $\mu_i^{IC} = \mu_i^{vapor}$, where now i stands for H_2 or D_2. The partition functions and the chemical potentials of each species consist of the same factors, but their meanings are different. For example, the rotational partition function is given now by the composite partition function ($Eqs.11, 12$) of each isotope. Since the H_2 and D_2 species have different masses, their zero point energies will be different, and these will give a nontrivial contribution to the selectivity (as will differences in the rotational energies). The transverse CM oscillations of the molecule in the IC or grooveare treated as excitations of a 2D harmonic oscillator. The corresponding partition function is:

$$q_{vib} = [\sum_{n=0}^{\infty} e^{-\beta\hbar\omega(n+1/2)}]^2 = \frac{e^{-\beta\hbar\omega}}{(1 - e^{-\beta\hbar\omega})^2} \tag{19}$$

where ω is the frequency of CM oscillations, found from the force constant. The rotational hindrance is expressed in terms of the rotational energy shifts,

ϵ_{mj} and the additive constants (C) in the expansion of the rotational part of the interaction potential [35]. This additive (reference) energy is also diferent for D_2 and H_2. The rotational hindrance leads to a shift of the binding energy of each species: $E_b = -(C + \hbar\omega + \epsilon_{00})$.

The equilibrium condition for each species ($i = D_2, H_2$) yields the ratio of IC (ρ_i) and vapor (n_i) densities for each species, which is then used to find the isotope selectivity.

$$\frac{\rho_i}{n_i} = \lambda_i^2 \frac{\exp\left(-\beta\hbar\omega_i\right)}{(1-\exp\left(-\beta\hbar\omega_i\right))^2} \frac{\exp\left(-\beta C\right) q_{rot}^{IC}}{q_{rot}^{free}} \tag{20}$$

The isotope selectivity is:

$$S_0 = \frac{\rho_{D_2}/\rho_{H_2}}{n_{D_2}/n_{H_2}} \tag{21}$$

$Eq.20$ implies that at low T the main contribution to selectivity comes from the difference between the binding energies

$$S_0 \approx \frac{1}{2} \exp\left[-\beta(C_{D_2} + \hbar\omega_{D_2} + \epsilon_{00}^{D_2} - C_{H_2} - \hbar\omega_{H_2} - \epsilon_{00}^{H_2})\right] = \frac{1}{2} exp[\beta(E_b^{D_2} - E_b^{H_2})] \tag{22}$$

Fig.5 displays the results of our calculations for isotopic selectivity in the ICs and grooves of an (18,0) nanotube bundle, and on graphite (for comparison). All three surfaces favor D_2. However, the isotope selectivity in the IC and groove is much larger than that on graphite and within the tubes [25]. Even at 300 K the selectivity in the IC and groove is substantial, due to the large difference between the D_2 and H_2 binding energies. This large difference comes primarily from the zero point energy (but the difference between the rotational energies also contributes). Table 1 presents our results for the different contributions to the the binding energies. The difference between D_2 and H_2 binding energies is ~ 400 K in the IC and ~ 170 K in the groove, much larger than the difference of ~ 35 K on graphite [39]. When exponentiated, these differences lead to the very large selectivities found in the IC and groove. We may compare our results with previous calculations. Challa *et al.* have studied isotope selectivity at variable pressure in the interstices of (10,10) nanotube bundle, using Ideal Adsorbed Solution Theory(IAST) and Path Integral Grand Canonical Monte Carlo simulations (PI-GCMC) [25]. At low pressures, the IAST and PI-GCMC results converge to the analytic zero pressure results. In their calculation, only the transverse zero-point energy is considered, i.e. rotational motion is ignored. The selectivity calculated

by them at 20 K and very low pressure (10^{-13} atm) is about 700. (10,10) and (18,0) nanotubes have similar diameters (13.6 and 13.8, respectively), so the interstices of a closed packed nanotube bundle are similar, too (~ 6 $\mathring{A}$ diameter). Recently, Hathorn *et al.* [45] have estimated the quantum effects due to the restriction of the rotational motion of H_2 and D_2 adsorbed within a single nanotube. Their results reveal significantly enhanced rotational separation factor(selectivity), which at 20 K is of order 10^3. The zero pressure isotope selectivity calculated by us at 20 K, in the interstices of bundles of (18,0) carbon nanotubes is of order 10^9. Our results differ to such a large degree since we considered both zero point and rotational contributions to selectivity and we used a slightly deeper, solid-fluid potential. The stronger the confinement, the larger the difference between the isotope zero point energies and between the rotational energies. Previous calculations inside (5,5) nanotubes at 20 K yielded much lower isotope selectivities [26]. At low pressure, the computed selectivity of tritium to H_2 is 23, and that of tritium to D_2 is 1.7; hence $S_0(D_2/H_2) = 13$. Thus, even if the inner channels of (5,5) nanotubes have about the same radius (3.3 $\mathring{A}$) as the ICs of (18,0) nanotube bundles (3 $\mathring{A}$), the computed selectivity in the IC is much larger due to the different arrangement of the carbon atoms in the IC, which yields greater confinement.

5 Isosteric heat

The isosteric heat is defined as:

$$Q_{st} = -[\frac{d(lnP)}{d\beta}]_N \tag{23}$$

where P is the pressure of the vapor outside the nanotube bundles. In our model, at low density, the dependence of P on T can be found from the equilibrium condition ($Eq.2$) using the ideal gas formula: $n = \beta P$. Finally, the isosteric heat is:

$$Q_{st} = 2k_BT - \hbar\omega - C + (\frac{d}{d\beta})[ln\frac{(q_{rot}^{IC}/q_{rot}^{free})}{(1-e^{-\beta\hbar\omega})^2}] \tag{24}$$

At low T, the excitations can be neglected and the term involving the derivative with respect to β goes to $-\epsilon_{00} - (\epsilon_{10} - \epsilon_{00})e^{-\beta(\epsilon_{10}-\epsilon_{00})} + 2Be^{-2\beta B}$,

where ϵ_{00} and ϵ_{10} are the first two rotational energy levels. Therefore, at low T, the isosteric heat is a measure of the binding energy:

$$Q_{st} = E_b + 2k_B T \tag{25}$$

since $E_b = -(C + \hbar\omega + \epsilon_{00})$.

The isosteric heat can be found experimentally by taking the difference between two nearby isotherms. Recently, there have been reported experiments of adsorption of D_2 and H_2 in carbon nanotube bundles [33], which show isosteric heats in nanotube bundles to be a factor of 1.5 (for H_2) to 1.8 (for D_2) larger than those on graphite. This means that the D_2 and H_2 binding energies are almost twice as large as those on graphite. Moreover, the difference between isotope isosteric heats, which again is related to the difference between isotope binding energies, was found to be about 200 K, much greater than the difference of about 35 K on graphite [39]. This is a mark of the greater confinement of molecules adsorbed in nanotube bundles than on the surface of graphite; the confinement leads to the enhanced separability of isotopes found in the previous section.

We performed calculations of the isotope isosteric heats in the low density limit (*Eq*.24). Table 2 and Figs. 6(a),(b) compare the results of the calculated isosteric heats and the low coverage experimental data at T=85 K. The experimental procedure of Wilson *et al* does not reveal where in the nanotube bundle the adsorption occurs. Since the experimental isosteric heats are much larger than on graphite, one assumes that the adsorption environment should be either the IC or the groove site. Our calculations of the isosteric heats in both IC and groove are lower than the experimental results. The calculated difference between D_2 and H_2 isosteric heats (374 K) in the IC is much larger than the one found experimentally, but the difference (137 K) in the groove is closer to the experimental difference (200 K). In addition, the calculated binding energies(see Table I) for D_2 and H_2 in the grooves are consistent with the experimental results and show that the adsorption on the grooves is much more likely than on the IC at low T. Assuming the accuracy of our approximations, we believe that our results are compatible with an adsorption in the groove, rather than the IC. This is also experimentally plausible, since the external grooves are more accessible for adsorption than the ICs. Indeed, the ICs may be completely blocked, preventing any adsorption there.

6 Summary and conclusions

We have investigated the spin (ortho versus para) and the isotope (D_2 versus H_2) selectivity at low coverage in the IC and groove channel of (18,0) nanotube bundles. The rotational hindrance of molecules in the IC and groove site induces shifts and splittings in the rotational spectrum, enabling the nanotube bundles to preferentially adsorb H_2 ortho molecules and D_2 para molecules. Our calculations show substantial spin selectivity for temperatures up to $\sim$ 100 K in the IC and up to $\sim$ 75 K in the groove. At low temperatures, the alterations of the rotational spectrum in the IC induces new features in the ortho heat capacity, as the ortho-ortho peak. The H_2 equilibrium heat capacity exhibits a distinctive ortho-para conversion peak at $\sim$ 20 K. The different features of non-equilibrium and equilibrium heat capacities may be a way to check the existence of the ortho-para conversion of H_2 and D_2 adsorbed in nanotube bundles. In the case of the isotope selectivity in nanopores, zero-point motion favors the heavier isotope [25], and the rotational motion enhances the preferential adsorption of the heavier isotope [35, 45]. We find substantial isotope selectivity even at temperatures as high as 300 K in the IC and groove. At 20 K, our calculation at low coverage (consequently zero pressure) yield isotope selectivities of order 10^9 in the IC, orders of magnitude larger than the low pressure limit found in the calculations of Wang *et al.* and Challa *et al.*. Our much larger isotope selectivity is a consequence of the stronger confinement in the IC, which yields larger zero point and rotational energies. The difference between the D_2 and H_2 isosteric heats in the groove ($\sim$ 135 K) is close to the value found experimentally ($\sim$ 200 K). We conclude that carbon nanotube bundles are ideal surfaces for spin and isotope separation, providing a potential technology of quantum sieving.

We acknowledge stimulating discussions with J. K. Johnson, M. M. Calbi, T. Wilson, M. J. Bojan, O. Vilches, P. Sokol, D. Narehood and D. Stojkovic. This research has been supported by Petroleum Research Foundation of the American Chemical Society and Air Products and Chemicals, Inc.

References

[1] A.C. Dillon, K.M. Jones, T.A. Bekkedahl, C.H. Kiang, D.S. Bethune and M.J. Heben, *Nature* **386**, 337 (1997).

[2] P. Chen, X. Wu, J. Lin and K.L. Tan, *Science* **285**, 91 (1999).

[3] Y. Ye, C.C. Ahn, C. Witham, B. Fultz, J. Liu, A.G. Rinzler, D. Colbert, K.A. Smith and R.E. Smalley, Appl. Phys. Lett. **74**, 16 (1999).

[4] Q. Wang, J.K. Johnson, J. Phys. Chem. B **103**, 4809 (1999).

[5] Q. Wang, J.K. Johnson, J. Chem. Phys. **110**, 577 (1999).

[6] V.V. Simonyan, P. Diep, J.K. Johnson, J. Chem. Phys. **111**, 9778 (1999).

[7] V. Meregalli, M. Parrinello, Appl. Phys. **A** 72, 143 (2001).

[8] S. Inoue, N. Ichikuni, T. Suzuki, T. Uematsu and K. Kaneko, J. Phys. Chem B **102**, 4689 (1998).

[9] G. Gao, T. Cagin and W.A. Goddard III, Phys. Rev. Lett. **80**, 5556 (1998).

[10] Y.F. Yin, T. Mays and B. McEnaney, Langmuir **15**, 8714 (1999).

[11] A. Kuznetsova, J.T. Yates,Jr., J. Liu and R.E. Smalley, J. Chem. Phys. **112**, 9590 (2000).

[12] K.A. Williams and P.C. Eklund, Chem. Phys. Lett. **320**, 352 (2000).

[13] M.S. Dresselhaus, K.A. Williams and P.C. Eklund, MRS Bulletin, **24**, 45 (1999).

[14] G. Stan and M.W. Cole, J. Low Temp. Phys. **110**, 539 (1998).

[15] M.W. Cole, V.H. Crespi, G. Stan, C. Ebner, J.M. Hartman, S. Moroni and M. Boninsegni, Phys. Rev. Lett. **84**, 3883 (2000).

[16] G. Stan, M.J. Bojan, S. Curtarolo, S.M. Gatica and M.W. Cole, Phys. Rev. B **62**, 2173 (2000).

[17] H. Cheng, G.P. Pez and A.C. Cooper, J. Am. Chem. Soc. **123**, 5845 (2001).

[18] A. Thess, R. Lee, P. Nikolaev *et al.* , *Science* **273**, 483 (1996).

[19] R.R. Schlittler, J.W. Seo, J.K. Gimzewski, C. Durkan, M.S.M. Saitfullah and M.E. Welland, *Science* **292**, 1136 (2001).

[20] S.B. Sinnott and R. Andrews, Crit. Rev. Solid State Mater. Sci. **26**, 145 (2001).

[21] D. Goulding, J.P. Hansen and S. Melchionna, Phys. Rev. Lett. **85**, 1132 (2000).

[22] A.A. Lucas, F. Moreau, P. Lambin, Rev. Mod. Phys. **74**, 1 (2002).

[23] K.A. Williams, B.K. Pradhan, P.C. Eklund, M.K. Kostov and M.W. Cole, Phys. Rev. Lett. **88**, 165502 (2002).

[24] Q. Wang, S.R. Challa, D.S. Sholl and J.K. Johnson, Phys. Rev. Lett. **82**, 956 (1999).

[25] S.R. Challa, D.S. Sholl, and J.K. Johnson, J. Chem. Phys. **116**, 814 (2002).

[26] M.C. Gordillo, J. Boronat and J. Casulleras, Phys. Rev. B. **65**, 014503 (2001).

[27] *McGraw-Hill Encyclopedia of Science and Technology*, 8 ed. (Mc.Graw-Hill, New York 1997), Vol.9 .

[28] P.T. Greenland, Contemp. Phys. **30**, 405 (1990).

[29] I.S. Averbukh, M.J.J. Vrakking, D.M. Villeneuve and A. Stolow, Phys. Rev. Lett. **77**, 3518 (1996).

[30] R.S. Hansen, J. Phys. Chem. **63**, 743 (1959).

[31] D. Basmadjian, Can. J. Chem. **38**, 141 (1960).

[32] D. Basmadjian, Can. J. Chem. **38**, 149 (1960).

[33] F. Stephanie-Victoire, A.-M. Goulay and E. C. de Lara, Langmuir **14**, 7255 (1988).

[34] J.J.M. Beenakker, V.D. Borman and S. Yu. Krylov, Chem. Phys. Lett. **232**, 379 (1995).

[35] M.K. Kostov, H. Cheng, R.M. Herman, M.W. Cole and J.C. Lewis, J. Chem. Phys. **116**, 1720 (2002).

[36] D.G. Narehood, M.K. Kostov, P.C. Eklund, M.W. Cole and P.E. Sokol, Phys. Rev. B **65**, 233401 (2002) .

[37] T. Wilson, A. Tyburski, M.R. DePies, O.E. Vilches, D. Becquet and M. Bienfait, J. Low Temp. Phys. **126**, 403 (2002).

[38] C.M. Brown, T. Yildirim, D.A. Neumann, M.J. Heben, T. Gennet, A.C. Dillon, J.L. Alleman, and J.E. Fisher, Chem. Phys. Lett. **329**, 311-316 (2000).

[39] G. Vidali, G. Ihm, H-Y Kim, and M.W. Cole, Surf. Sci. Reports **12**, 135 (1991).

[40] S.E. Weber, S. Talapatra, C. Journet, A. Zambano, A.D. Migone, Phys. Rev. B **61**, 13150 (2000).

[41] D. Stojkovic, private communications.

[42] A.C. Dillon, M.J. Heben, Appl. Phys. A **72**, 133 (2001).

[43] Y. Ye, C.C. Ahn, C. Witham, B. Fultz, J. Liu, D. Colbert, K.A. Smith, R.E. Smalley, Appl. Phys. Lett. **74**, 2307 (1999).

[44] In constrast, S.A. FitzGerald, S. Forth and M. Rinkoski, Phys.Rev.B **65**, 140302 (2002), found a shifted internal vibrational energy of H_2 in fullerite.

[45] B.C Hathorn, B.G. Sumpter and D.W. Noid, Phys.Rev.A **64**, 022903 (2001).

[46] M.W. Cole, V.H. Crespi, G. Stan, C. Ebner, J.M. Hartman, S. Moroni, and M. Boninsegni, Phys. Rev. Lett. **84**, 3883 (2000).

[47] M. Boninsegni, S.Y. Lee and V.H. Crespi, Phys. Rev. Lett. **86**, 3360 (2001).

[48] The reference energy is the first term in the expansion of the rotational part of the confining potential: $V = C + C_2 cos^2\theta + C_4 cos^4\theta$. The minimum of the potential $(C + C_2 + C_4)$ is the same for H_2 and D_2, but their expansion terms C_i are different since they have been derived after averaging the holding potential over the zero point motion of H_2 and D_2. For more details see Ref. 35.

[49] Similar shifts and splittings of the rotational spectrum have been found previously by Hathorn *et al.* inside nanotubes [45].

Table 1: The zero point energies ($\hbar\omega$), rotational energy references (C) and shifts (ϵ_{00}) and binding energies (E_b) (expressed in Kelvin). $D_2 - H_2$ means the difference between the corresponding values.

	$\hbar\omega^{IC}$	$\hbar\omega^{groove}$	C^{IC}	C^{groove}	ϵ_{00}^{IC}	ϵ_{00}^{groove}	E_b^{IC}	E_b^{groove}	$E_b^{graphite}$
D_2	762	266	-1445	-970	-133	-62	816	766	517
H_2	1077	370	-1278	-880	-206	-93	407	603	482
$D_2 - H_2$	-315	-114	-166	-90	73	31	409	163	35

Table 2: The isotope isosteric heats (Q) in the IC, groove and experimental results (expressed in Kelvin)

	Q_{calc}^{IC}	Q_{calc}^{groove}	Q_{exp}
D_2	991	901	1100±90
H_2	617	764	900±70
$D_2 - H_2$	374	137	200±110

Figure captions

Fig. 1. H_2 rotational spectrum in free space and in IC. The number of lines in a level represents the degeneracy of that energy level. o and p mean ortho and para, respectively.

Fig. 2. D_2 and H_2 spin selectivity in IC and groove channel as a function of T

Fig. 3. Ortho (dashed line), para (dotted line) and non-equilibrium (full line) specific heat (without spin equilibration) of H_2 molecules (a) in IC, (b) in free space

Fig. 4. The equilibrium rotational specific heat of H_2 (full line) and of D_2 (dashed line)

Fig. 5. Isotope selectivity in the IC (full line), groove (dashed line) and on graphite (dotted line).

Fig. 6. The calculated H_2 (dotted line), D_2 (dashed line) and the difference $D_2 - H_2$ (full line) isosteric heats (a) in the IC and (b) in the groove. The experimental values at 85 K are shown in symbols: circle for D_2, square for H_2 and triangle for the difference $D_2 - H_2$.

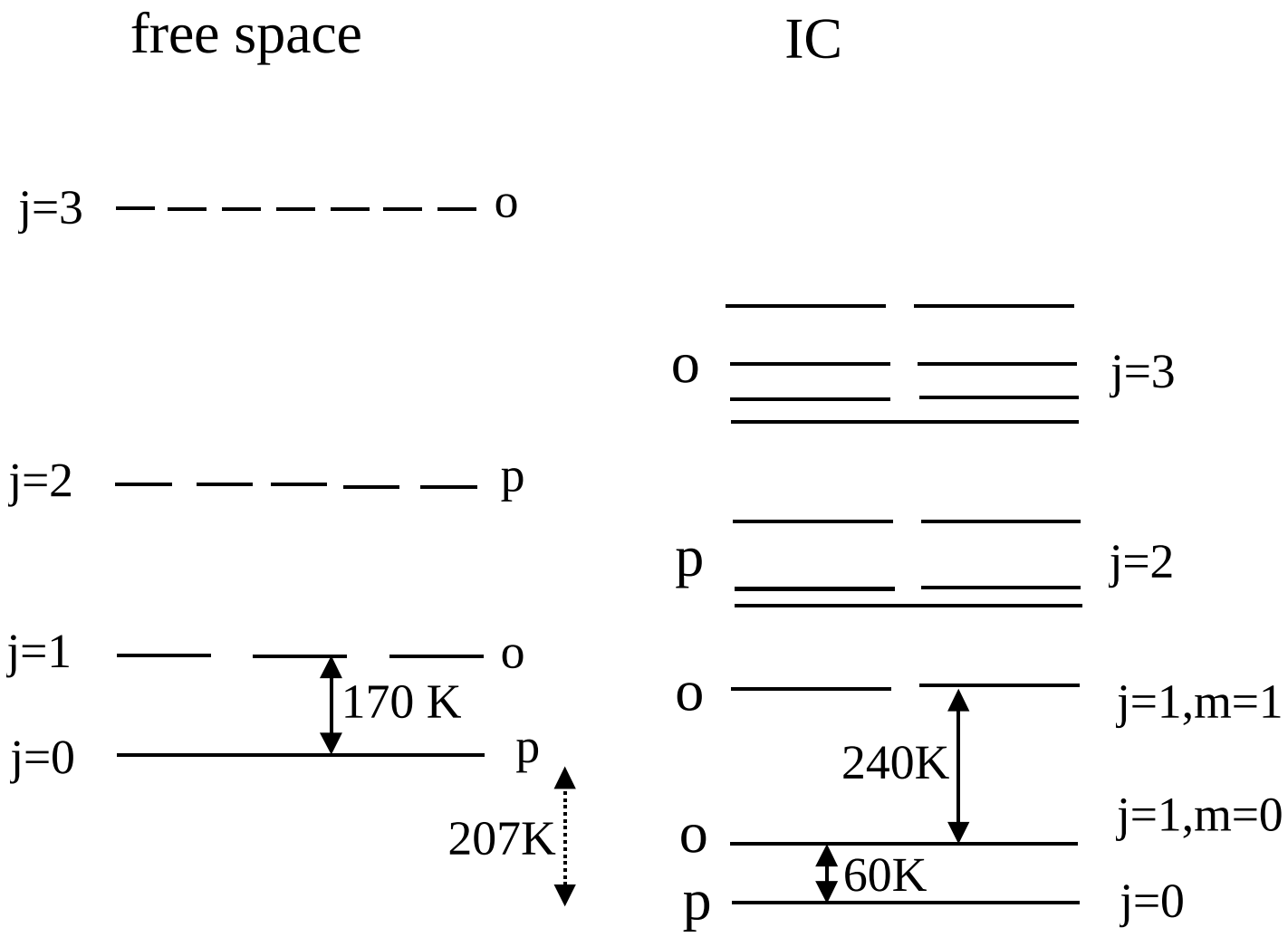
free space
IC
j=3
o
j=2
p
j=1
o
170 K
j=0
p
207K
o
j=3
p
j=2
o
j=1,m=1
240K
o
j=1,m=0
60K
p
j=0

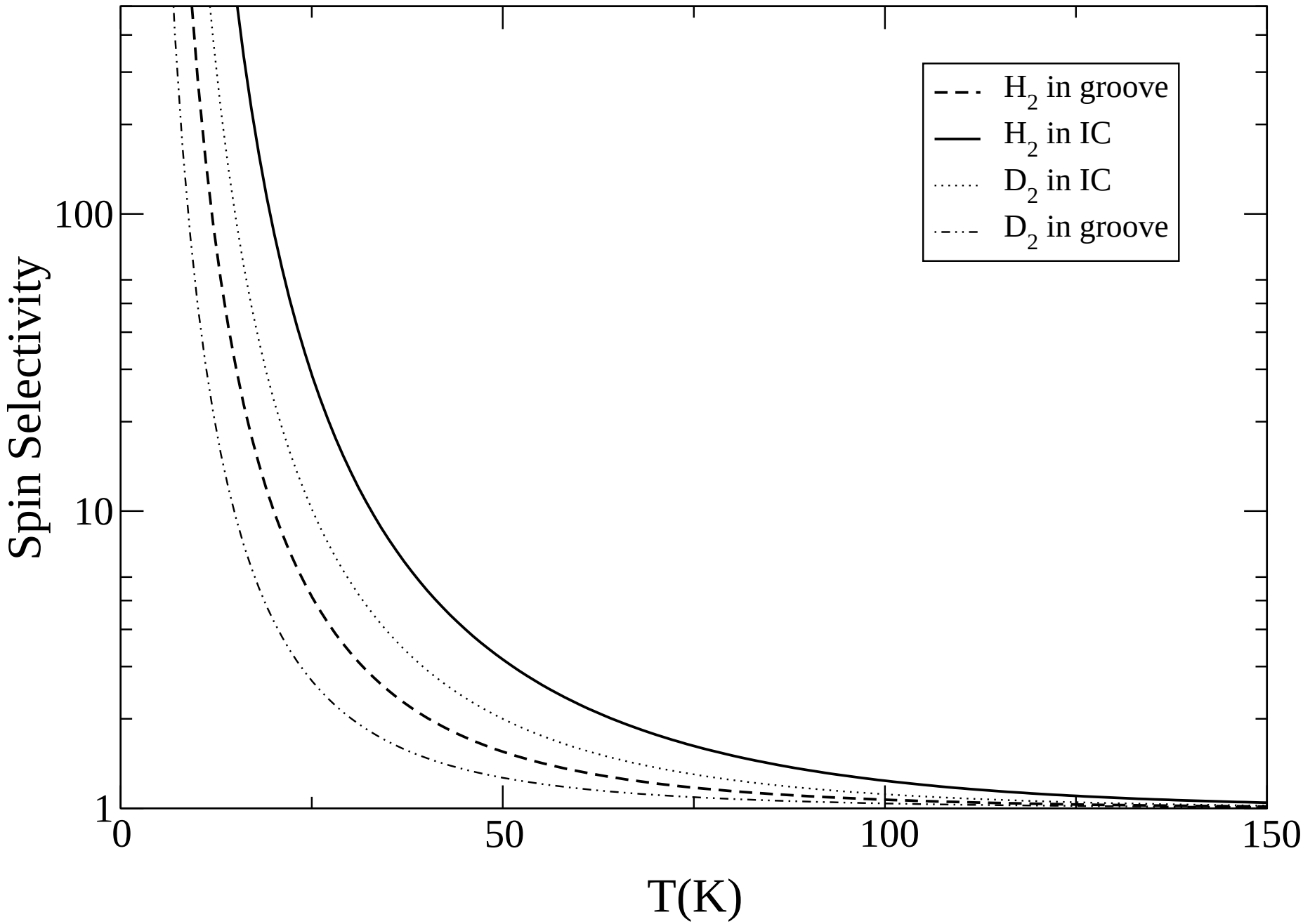
Spin Selectivity
100
10
1
0
50
100
150
T(K)
H2 in groove
H2 in IC
D2 in IC
D2 in groove

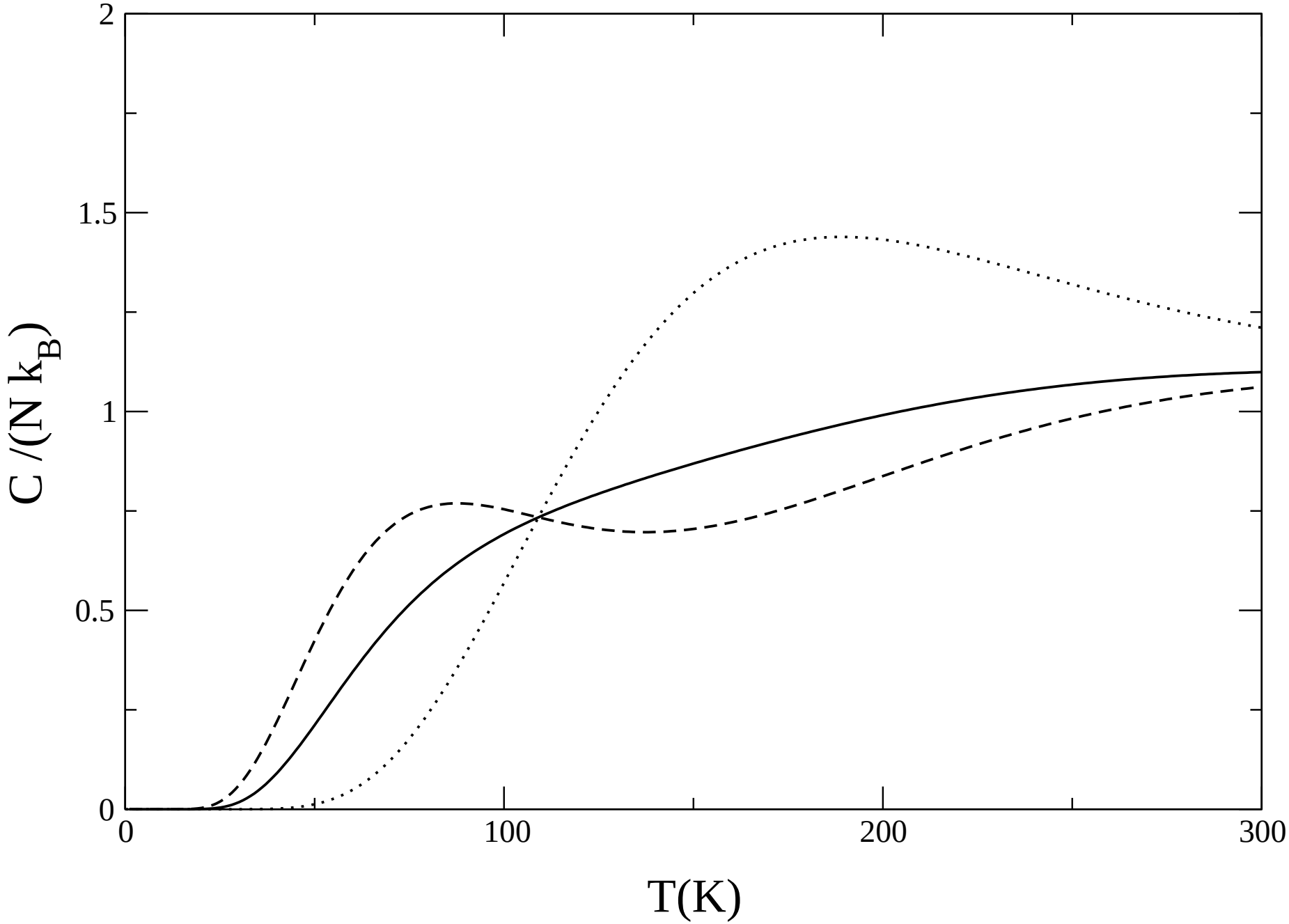
2
1.5
1
0.5
0
0
100
200
300
C /(N k_B)
T(K)

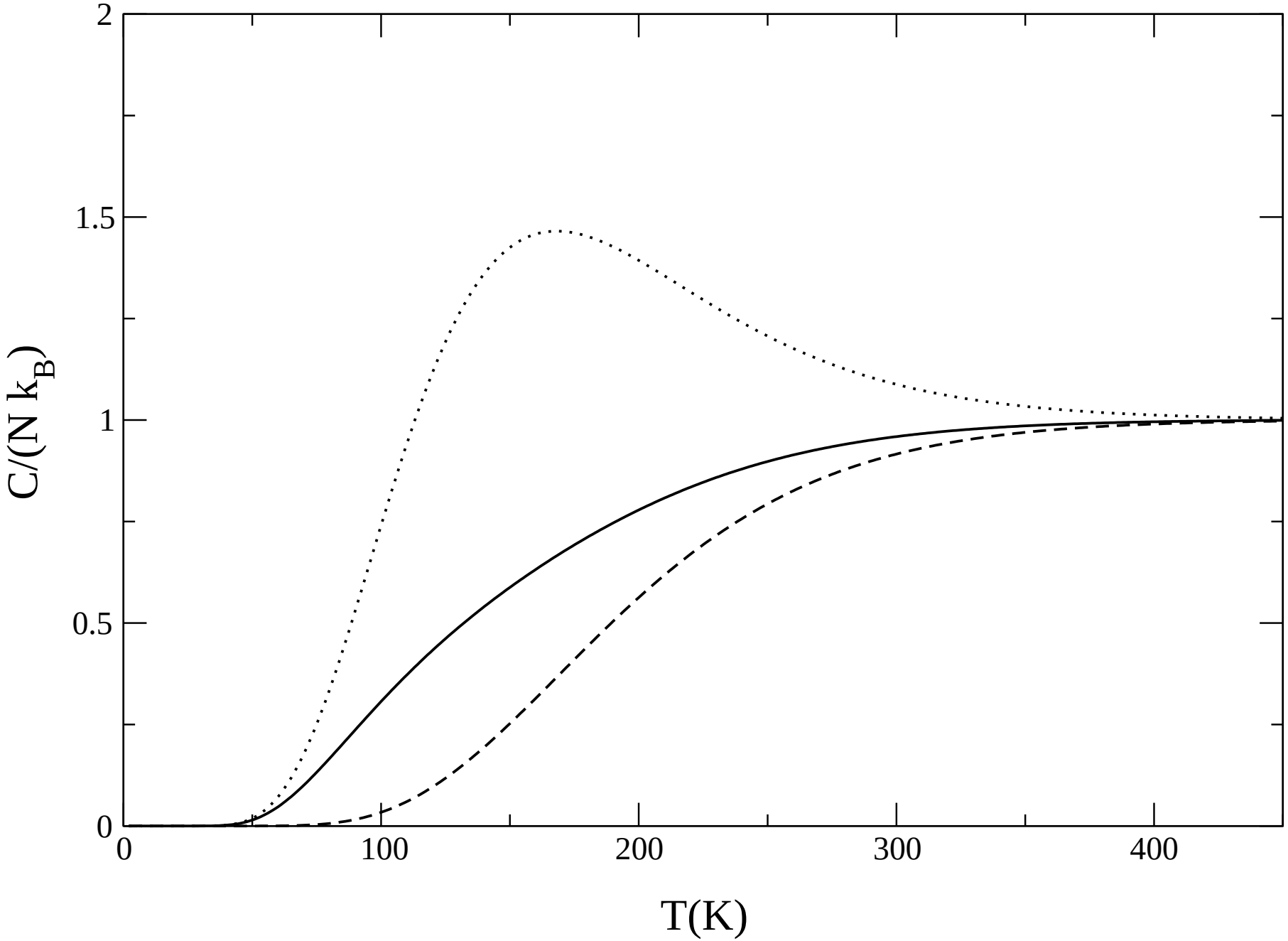
2
1.5
1
0.5
0
0
100
200
300
400
C/(N k_B)
T(K)

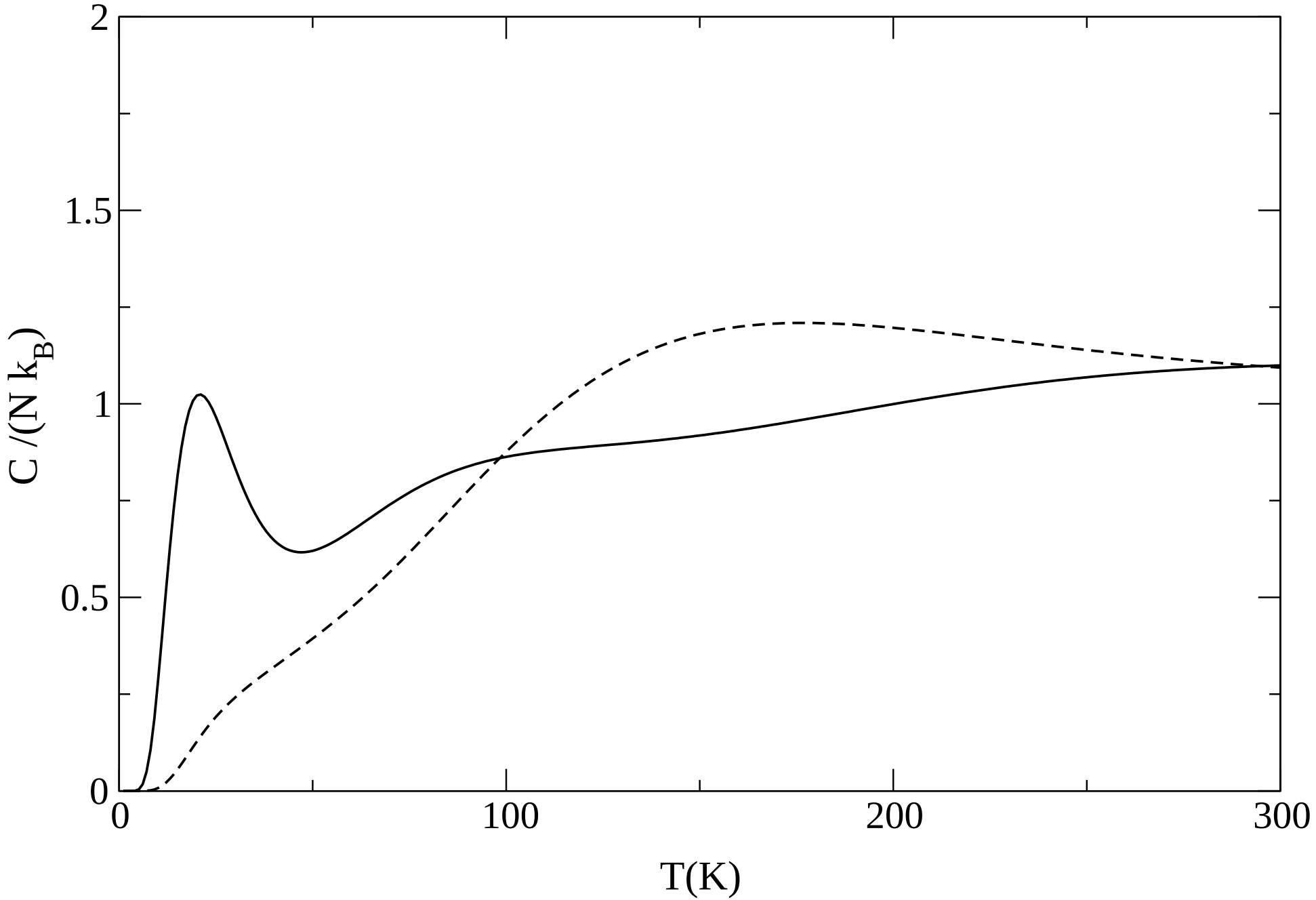
2
1.5
1
0.5
0
C /(N k_B)
0
100
200
300
T(K)

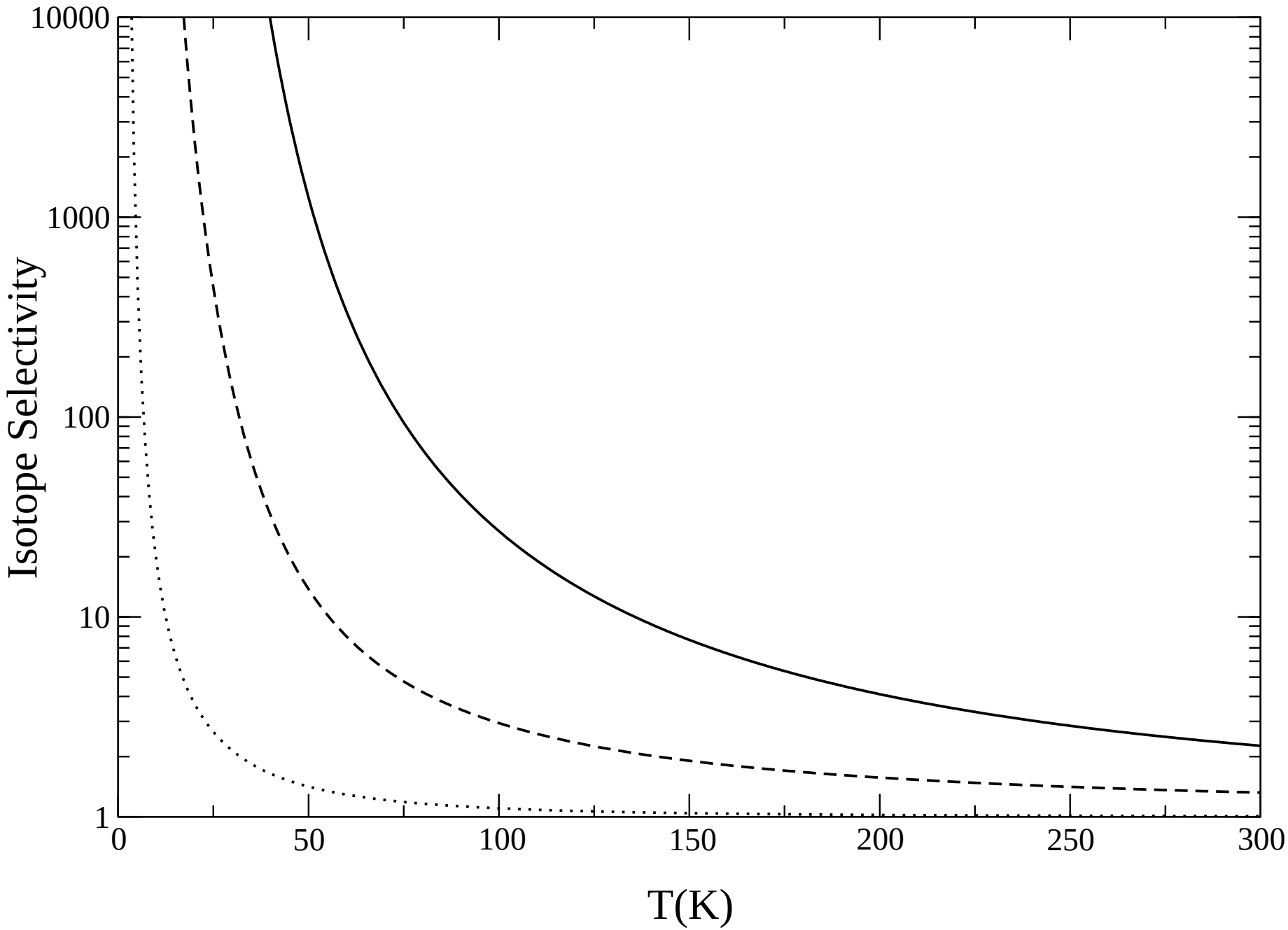
10000
1000
100
10
1
Isotope Selectivity
0
50
100
150
200
250
300
T(K)

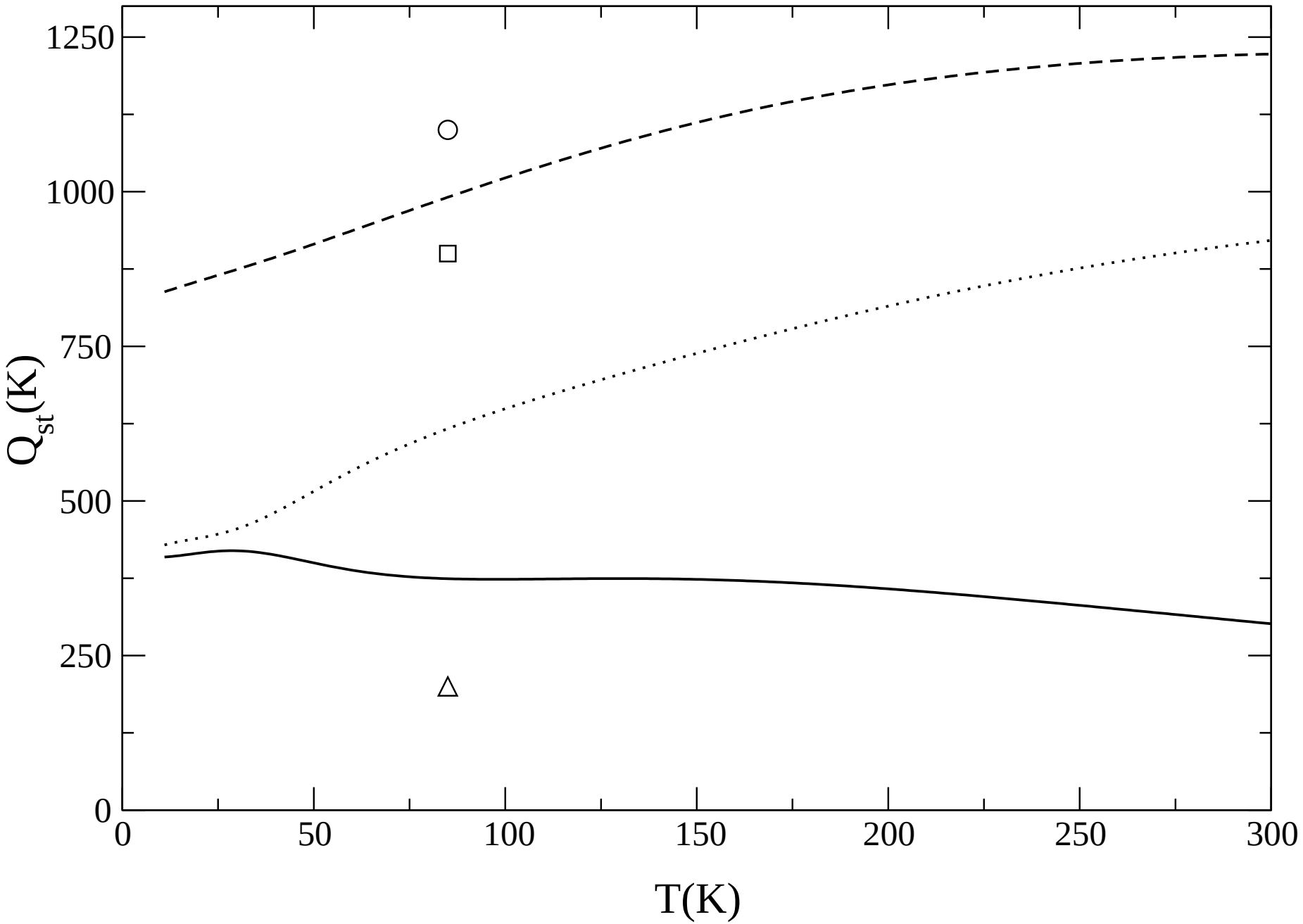
1250
1000
750
500
250
0
Q_{st}(K)
0
50
100
150
200
250
300
T(K)

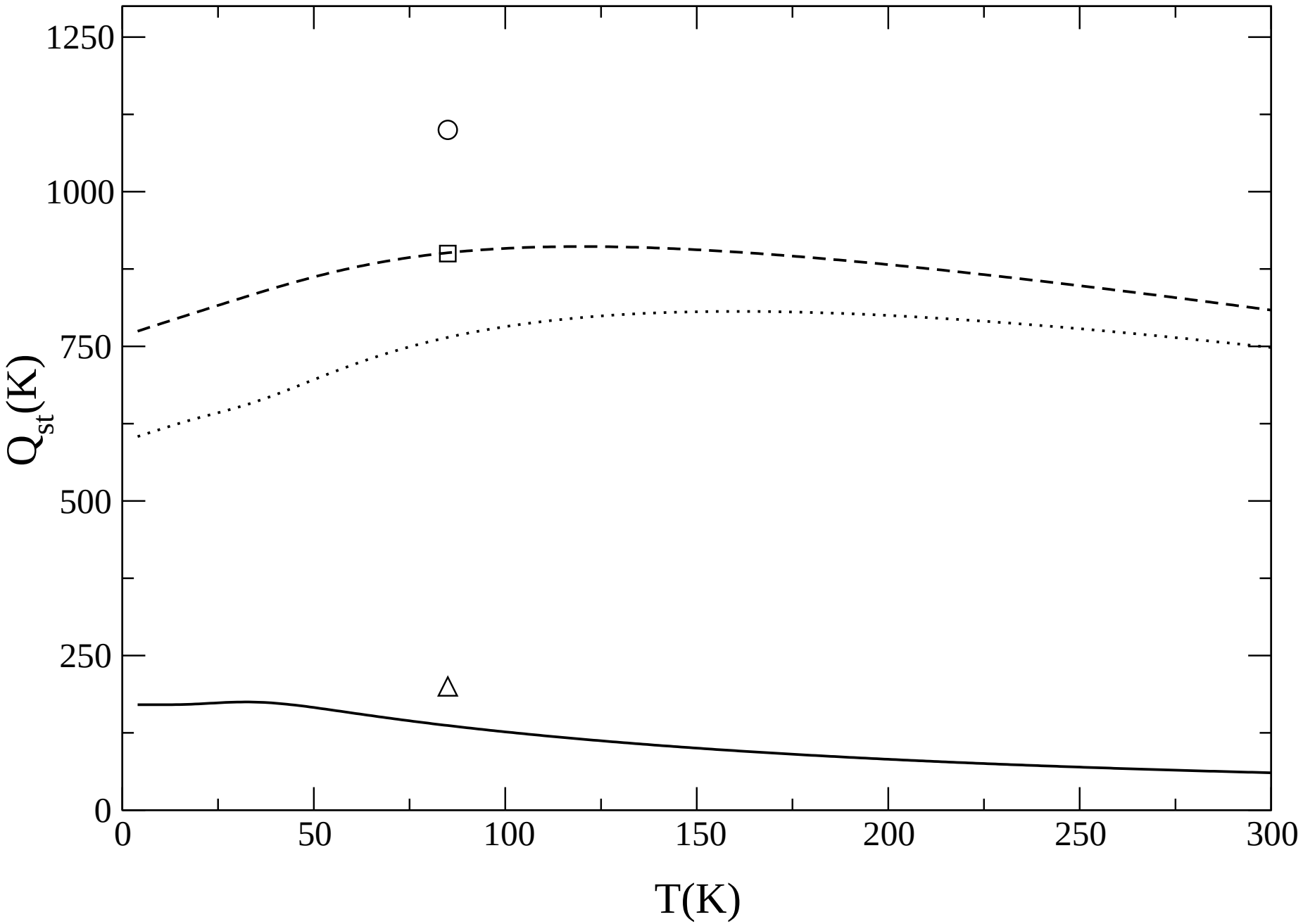
1250
1000
750
500
250
0
Q_{st}(K)
0
50
100
150
200
250
300
T(K)